

Thomas Droß and Robert
Glaum*Institut für Anorganische Chemie, Rheinische
Friedrich-Wilhelms-Universität Bonn, Gerhard-
Domagk-Straße 1, D-53121 Bonn, Germany

Correspondence e-mail: rglaum@uni-bonn.de

Key indicators

Single-crystal X-ray study
 $T = 293\text{ K}$
Mean $\sigma(\text{P}-\text{O}) = 0.004\text{ \AA}$
Disorder in solvent or counterion
 R factor = 0.027
 wR factor = 0.059
Data-to-parameter ratio = 15.2For details of how these key indicators were
automatically derived from the article, see
<http://journals.iucr.org/e>.The langbeinite-type barium vanadium(III)
orthophosphate, $\text{Ba}_3\text{V}_4(\text{PO}_4)_6$ Langbeinite-type $\text{Ba}_3\text{V}_4(\text{PO}_4)_6$ has been crystallized from a stoichiometric melt starting from $\text{Ba}(\text{PO}_3)_2$ and V_2O_3 . The crystal structure has been refined from single-crystal X-ray diffraction data. It consists of a vanadato(III)–phosphate network $[\text{V}_4(\text{PO}_4)_6]^{6-}$, which shows some resemblance to the NASICON structure type. A new method is presented for the visualization of this structural relationship. The single-crystal electronic spectrum of yellow–green $\text{Ba}_3\text{V}_4(\text{PO}_4)_6$ shows the absorption bands typical for the octahedral chromophore $[\text{V}^{\text{III}}\text{O}_6]$.

Received 27 February 2004

Accepted 10 March 2004

Online 20 March 2004

Comment

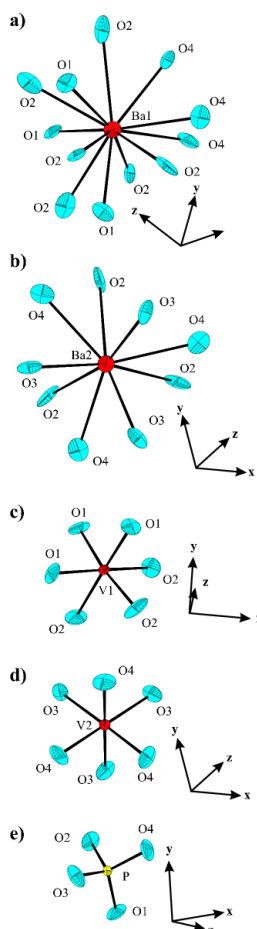
Quaternary diphosphates $AM^{\text{II}}\text{P}_2\text{O}_7$ (A : Ca, Sr, Ba; M^{II} : Mg, Cr–Zn) allow stabilization of transition metals in compara-

Figure 1

Coordination polyhedra (a) $[\text{Ba1O}_{12}]$, (b) $[\text{Ba2O}_9]$, (c) $[\text{V1O}_6]$, (d) $[\text{V2O}_6]$ and (e) $[\text{PO}_4]$, showing displacement ellipsoids at the 74% probability level and the atom numbering.

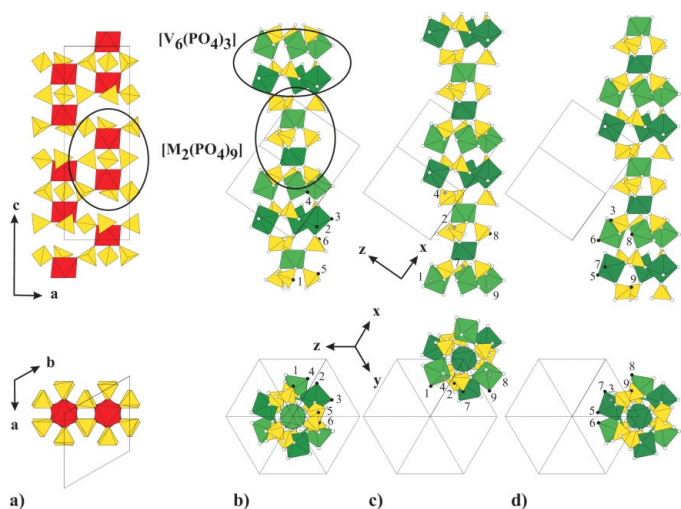


Figure 2

Comparison of the NASICON structure (a) with the langbeinite-type structure (b)–(d) of $\text{Ba}_3\text{V}_4(\text{PO}_4)_6$. Filled numbered dots mark O atoms (in front of the illustration) linking adjacent columns. Building units $[\text{M}_2(\text{PO}_4)_9]$ ($M = \text{Zr}, \text{V}$) and $[\text{V}_6(\text{PO}_4)_3]$ are highlighted. Colour key: grey shaded dots represent eclipsed oxygen links; red: $[\text{MO}_6]$ groups in the NASICON structure; light green: $[\text{V1O}_6]$; dark green: $[\text{V2O}_6]$; yellow: $[\text{PO}_4]$.

tively low oxidation states [e.g. Cr^{2+} : CaCrP_2O_7 (Maaß *et al.*, 2001), SrCrP_2O_7 (Maaß & Glaum, 2000), BaCrP_2O_7 (Maaß *et al.*, 2001); Fe^{2+} : CaFeP_2O_7 (Maaß, 2002), SrFeP_2O_7 (le Meins & Courbion, 1999), BaFeP_2O_7 (Maaß, 2002)]. See El Bali *et al.* (2001) and Maaß (2002) for a complete survey of the $\text{AM}^{\text{II}}\text{P}_2\text{O}_7$ family.

Aiming at the synthesis of $\text{BaV}^{\text{II}}\text{P}_2\text{O}_7$, we obtained $\text{Ba}_3\text{V}_4(\text{PO}_4)_6$. This quaternary orthophosphate belongs to the large langbeinite (Zemann & Zemann, 1957) structure family. In addition to several sulfates (Speer & Salje, 1986; Moriyoshi & Itoh, 1996; Guelylah, Breczewski & Madariaga, 1996; Guelylah, Madariaga & Breczewski, 1996), many phosphates $\text{A}_2\text{M}_2(\text{PO}_4)_3$ (A : alkali or alkaline earth metal, M : tri- or tetravalent transition metal or rare earth metal) (Battle *et al.*, 1986, 1988; Norberg, 2002; Albina *et al.*, 2003) and one fluoroberyllate $\text{K}_2\text{Mn}_2(\text{BeF}_4)_3$ (Guelylah, Breczewski & Madariaga, 1996) belong to this structure family.

The crystal structure of $\text{Ba}_3\text{V}_4(\text{PO}_4)_6$ might be rationalized as a vanadato(III)–phosphate network $[\text{V}_4(\text{PO}_4)_6]^{6-}$ with Ba^{2+} ions in interstices for charge balance. Taking into account all O atoms closer to Ba than the nearest cation, 12-fold coordination is observed for Ba1 with a rather irregularly shaped coordination polyhedron, while Ba2 forms nine bonds; in this case, the coordination polyhedron might be described as a triply capped octahedron (Fig. 1). The crystal structure of $\text{Ba}_3\text{V}_4(\text{PO}_4)_6$ is just one of a few examples of a langbeinite-type compound with incomplete occupation of the A sites [compare with $\text{K}_{2-x}\text{Ti}_2(\text{PO}_4)_6$ (Leclaire *et al.*, 1989)].

From our refinement, only a slight preference of Ba^{2+} for site Ba1 over Ba2 could be detected. V^{3+} ions are octahedrally coordinated by oxygen from six phosphate groups. The crys-

tallographic site symmetry of both chromophores $[\text{V}^{\text{III}}\text{O}_6]$ belongs to point group C_3 . However, the $[\text{V1O}_6]$ octahedra show slightly higher angular distortion, as is generally observed for the M1 coordination in other langbeinite structures (Figs. 1c and 1d). The $[\text{PO}_4]$ groups form almost ideal tetrahedra (Fig. 1e). Despite its cubic symmetry, the three-dimensional structure of the langbeinite $[\text{V}_4(\text{PO}_4)_6]^{6-}$ network is quite difficult to describe. A reasonable approach, which we favour, uses a comparison between the crystal structures of the NASICON $\text{NaZr}_2(\text{PO}_4)_3$ (space group $R\bar{3}c$) (Hagman & Kierkegaard, 1968) and langbeinite structure types (Fig. 2). Both structures might be regarded as transition metal phosphate frameworks with large low-charged cations occupying interstices. For both frameworks, the transition metal–phosphate ratio is 2:3. In addition to these formal similarities, anionic building units $[\text{M}_2(\text{PO}_4)_9]$ ($M = \text{Zr}^{4+}$ in NASICON, V^{3+} in the described langbeinite) occur in both structures (Fig. 2).

In projections of the cubic langbeinite structure along and perpendicular to $[111]$, one can recognize columns built from $[\text{VO}_6]$ and $[\text{PO}_4]$ groups having a translational period of one cube diagonal. Within these columns, anionic $[\text{V}_2(\text{PO}_4)_9]^{21-}$ building units and cationic $[\text{V}_6(\text{PO}_4)_3]^{9+}$ units alternate, giving to these columns an overall composition $[\text{V}_8(\text{PO}_4)_{12}]^{12-}$ or $[\text{V}_4(\text{PO}_4)_6]^{6-}$. Perpendicular to $[111]$, these columns are linked by V–O–P bridges. Relative to the central column, adjacent columns are shifted $\frac{1}{2}$ or $\frac{\sqrt{2}}{2}$ of the translational period along $[111]$. In contrast to the NASICON structure type, the presence of the $[\text{V}_6(\text{PO}_4)_3]^{9+}$ units in the langbeinite structure allows formation of voids large enough to house cations of much bigger size than Na^+ . The electronic spectrum of $\text{Ba}_3\text{V}_4(\text{PO}_4)_6$ shows transitions at $14\,100\text{ cm}^{-1}$ (${}^3T_{1g} \rightarrow {}^3T_{2g}$) and $21\,900\text{ cm}^{-1}$ [${}^3T_{1g} \rightarrow {}^3T_{2g}(P)$]. Modelling of the transition energies within the framework of the angular overlap model (Jørgensen *et al.*, 1963; Richardson, 1993; Figgis & Hitchman, 2000) leads to good agreement with the observed transitions [$B = 596\text{ cm}^{-1}$, $C/B = 4.8$, $e_\sigma(\text{mean}) = 7750\text{ cm}^{-1}$, $e_\pi = \frac{1}{4}e_\sigma$]. The resulting bonding parameters compare well with those of $\text{VP}_3\text{SiO}_{11}$ (Droß, 2004), $\text{V}(\text{PO}_3)_3$, $\text{V}_4\text{P}_6\text{Si}_2\text{O}_{25}$ and $\text{V}_4(\text{P}_2\text{O}_7)_3$ (Glaum, 1999), which have been derived in earlier studies.

Experimental

Crystals of $\text{Ba}_3\text{V}_4(\text{PO}_4)_6$ were grown by melting a homogenized mixture of $\text{Ba}(\text{PO}_3)_2$ (150 mg, 0.5071 mmol) and V_2O_5 (50.67 mg, 0.3381 mmol) in a platinum crucible in air. The melt [$T_m = 1373$ (20) K] was rapidly heated, using an electrical furnace, to 1473 K, kept at that temperature for 1 h, cooled to 1073 K at a rate of 10 K h^{-1} and finally to room temperature at a rate of 50 K h^{-1} . After removing the crucible from the oven, the recrystallized melt was crushed and crystal fragments of the title compound were obtained. Microcrystalline single-phase powders were obtained from pellets (size $4 \times 4 \times 12\text{ mm}$) of the starting materials $\text{Ba}(\text{PO}_3)_2$ and V_2O_5 after heating for 3 d at 1323 K in sealed silica tubes ($L = 10\text{ cm}$ and $D = 1.6\text{ cm}$) in the presence of 30 mg iodine as mineralizer. Subsequent heating for 21 d yielded small yellow–green crystals of irregular shape.

Crystal data

Ba₃V₄(PO₄)₆
M_r = 1185.58
 Cubic, *P*2₁3
a = 9.8825 (7) Å
V = 965.16 (12) Å³
Z = 2
D_x = 4.08 Mg m⁻³
 Mo *K*α radiation

Cell parameters from 29 reflections
 $\theta = 2.9\text{--}30.0^\circ$
 $\mu = 8.49 \text{ mm}^{-1}$
T = 293 (2) K
 Cube, yellow-green
 0.1 × 0.1 × 0.1 mm

Data collection

Nonius KappaCCD diffractometer
 ψ and ω scans
 Absorption correction: numerical
 (*HABITUS*; Herrendorf, 1993)
T_{min} = 0.597, *T_{max}* = 0.707
 22 794 measured reflections
 930 independent reflections

930 reflections with *I* > 2σ(*I*)
R_{int} = 0.029
 $\theta_{\text{max}} = 30.0^\circ$
h = -13 → 13
k = -13 → 13
l = -13 → 13

Refinement

Refinement on *F*²
R[*F*² > 2σ(*F*²)] = 0.027
wR(*F*²) = 0.059
S = 1.13
 930 reflections
 61 parameters
w = 1/[σ²(*F_o*²) + 7.2584*P*]
 where *P* = (*F_o*² + 2*F_c*²)/3

(Δ/σ)_{max} = 0.015
 Δρ_{max} = 2.02 e Å⁻³
 Δρ_{min} = -1.90 e Å⁻³
 Extinction correction: *SHELXL97*
 Extinction coefficient: 0.0237 (15)
 Absolute structure: Flack (1983),
 393 Friedel pairs
 Flack parameter = -0.02 (3)

Table 1

Selected geometric parameters (Å, °).

Ba1—O1 ⁱ	2.843 (4)	V1—O2 ^{iv}	1.998 (4)
Ba1—O4 ⁱⁱ	2.961 (4)	V2—O4 ^v	1.996 (3)
Ba1—O2 ⁱ	3.047 (5)	V2—O3 ^{vi}	1.999 (3)
Ba1—O2 ⁱⁱ	3.225 (5)	P—O1	1.516 (3)
Ba2—O3	2.824 (4)	P—O4	1.521 (3)
Ba2—O4 ⁱ	3.009 (4)	P—O2	1.531 (4)
Ba2—O2 ⁱ	3.111 (4)	P—O3	1.534 (3)
V1—O1 ⁱⁱⁱ	1.983 (3)		
O1 ⁱⁱⁱ —V1—O1 ^{vii}	93.73 (16)	O4 ^v —V2—O4 ^{viii}	88.44 (17)
O1 ⁱⁱⁱ —V1—O2 ^{iv}	81.84 (18)	O4 ^v —V2—O3 ^{vi}	88.61 (15)
O1 ^{vii} —V1—O2 ^{iv}	92.35 (17)	O4 ^{viii} —V2—O3 ^{vi}	176.20 (17)
O1—V1—O2 ^{iv}	172.71 (18)	O4 ^{ix} —V2—O3 ^{vi}	89.08 (17)
O2 ^{iv} —V1—O2 ^{vi}	92.50 (16)	O3 ^{vi} —V2—O3 ^{iv}	93.75 (17)

Symmetry codes: (i) $\frac{1}{2} - z, 1 - x, y - \frac{1}{2}$; (ii) $-z, x - \frac{1}{2}, \frac{1}{2} - y$; (iii) z, x, y ; (iv) $1 - y, \frac{1}{2} + z, \frac{3}{2} - x$; (v) $1 - z, \frac{1}{2} + x, \frac{3}{2} - y$; (vi) $\frac{1}{2} + z, \frac{3}{2} - x, 1 - y$; (vii) y, z, x ; (viii) $\frac{3}{2} - y, 1 - z, \frac{1}{2} + x$; (ix) $\frac{1}{2} + x, \frac{3}{2} - y, 1 - z$.

The lattice parameters were refined with the program *SOS* (Soose, 1980), using 29 reflections from an image plate Guinier photograph. Site-occupation factors for Ba1 and Ba2 have been refined with and without a restraint on their sum; both results are identical within standard uncertainty [with SUMP: s.o.f.(Ba1) = 0.772 (2), s.o.f.(Ba2) = 0.727 (2); without SUMP: s.o.f.(Ba1) = 0.776 (4), s.o.f.(Ba2) = 0.732 (4)]. The maximum and minimum electron-density peaks are located 0.67 and 0.62 Å, respectively from Ba2..

Data collection: *COLLECT* (Nonius, 2001); cell refinement: *COLLECT* and *DENZO* (Otwinowski & Minor, 1997); data reduction: *COLLECT* and *DENZO*; program(s) used to solve structure: *SHELXS97* (Sheldrick, 1997); program(s) used to refine structure: *SHELXL97* (Sheldrick, 1997); molecular graphics: *ATOMS* (Dowty, 2002); software used to prepare material for publication: *WinGX* (Farrugia, 1999).

The authors thank Dr Jörg Daniels for the data collection.

References

Albina, I. O., Trubach, I. G., Kurazhkovskaya, V. S., Pertierra, P., Savado, M. A., Garcia-Granda, S., Khainakov, S. A. & Garcia, J. R. (2003). *J. Solid State Chem.* **173**, 314–318.
 Battle, P. D., Cheetham, A. K., Harrison, W. T. A. & Long, G. J. (1986). *J. Solid State Chem.* **62**, 16–25.
 Battle, P. D., Gibb, T. C., Nixon, S. & Harrison, W. T. A. (1988). *J. Solid State Chem.* **75**, 21–29.
 Dowty, E. (2002). *ATOMS for Windows*. Version 6.0. Shape Software, 521 Hidden Valley Road, Kingsport, TN 37663, USA.
 Droß, T. (2004). PhD thesis, University of Bonn, Germany.
 El Bali, B., Boukhari, A., Aride, J., Maaß, K. & Glaum, R. (2001). *Solid State Sci.* **3**, 669–676.
 Farrugia, L. J. (1999). *J. Appl. Cryst.* **32**, 837–838.
 Figgis, B. N. & Hitchman, M. A. (2000). *Ligand Field Theory and Its Applications*. New York: Wiley-VCH.
 Flack, H. D. (1983). *Acta Cryst.* **A39**, 876–881.
 Glaum, R. (1999). Habilitation thesis, University of Gießen, Germany. (URL: <http://bibd.uni-giessen.de/ghm/1999/uni/h990001.htm>.)
 Guelylah, A., Brezczewski, T. & Madariaga, G. (1996). *Acta Cryst.* **C52**, 2951–2954.
 Guelylah, A., Madariaga, G. & Brezczewski, T. (1996). *Acta Cryst.* **C52**, 2954–2956.
 Jørgensen, C. K., Pappalardo, R. & Schmidtke, H. H. (1963). *J. Chem. Phys.* **39**, 1422.
 Hagman, L. O. & Kierkegaard, P. (1968). *Acta Chem. Scand.* **22**, 1822–1832.
 Herrendorf, W. (1993). *HABITUS*. University of Karlsruhe, Germany.
 Leclaire, A., Benmoussa, A., Borel, M. M., Grandin, A. & Raveau, B. (1989). *J. Solid State Chem.* **78**, 227–231.
 Maaß, K. (2002). PhD thesis, University of Gießen, Germany. (URL: <http://bibd.uni-giessen.de/ghm/2002/uni/d020119.htm>.)
 Maaß, K. & Glaum, R. (2000). *Acta Cryst.* **C56**, 404–406.
 Maaß, K., Glaum, R. & Gruehn, R. (2001). *Z. Anorg. Allg. Chem.* **627**, 2081–2090.
 Meins, J.-M. le & Courbion, G. (1999). *Acta Cryst.* **C55**, 481–483.
 Moriyoshi, C. & Itoh, K. (1996). *J. Phys. Soc. Jpn.* **65**, 3537–3543.
 Nonius (2001). Collect. Nonius BV, Delft, The Netherlands.
 Norberg, S. T. (2002). *Acta Cryst.* **B58**, 743–749.
 Otwinowski, Z. & Minor, W. (1997). *Methods in Enzymology*, Vol. 276, *Macromolecular Crystallography*, Part A, edited by C. W. Carter Jr & R. M. Sweet, pp. 307–326. New York: Academic Press.
 Richardson, D. E. (1993). *J. Chem. Educ.* **70**, 372.
 Sheldrick, G. M. (1997). *SHELXS97* and *SHELXL97*. University of Göttingen, Germany.
 Soose, J. (1980). *SOS*. University of Gießen, Germany.
 Speer, D. & Salje, E. (1986). *Phys. Chem. Miner.* **13**, 17–24.
 Zemann, A. & Zemann, J. (1957). *Acta Cryst.* **10**, 409–413.